ELSEVIER

Thermochimica Acta 356 (2000) 143–151

thermochimica acta

www.elsevier.com/locate/tca

Heat capacity and thermochemical study of trifluoroacetamide ($C_2H_2F_3NO$)

You-Ying Di[a,b], Zhi-Cheng Tan[b,*], Xin-Ming Wu[a,b], Shuang-He Meng[b], Song-Sheng Qu[a]

[a]*College of Chemistry and Environmental Science, Wuhan University, Wuhan 430072, China*
[b]*Thermochemistry Laboratory, Dalian Institute of Chemical Physics, Chinese Academy of Sciences, Dalian 116023, China*

Received 4 January 2000; accepted 16 February 2000

Abstract

The low-temperature heat capacities of trifluoroacetamide were precisely determined with a small sample precision automated adiabatic calorimeter over the temperature range from 78 to 404 K. A solid-to-solid phase transition, a fusion and a phase transition from a liquid crystalline phase to fully liquid phase have been observed at the temperatures of 336.911±0.102, 347.622±0.094 and 388.896±0.160 K, respectively. The molar enthalpies of these phase transitions as well as the chemical purity of the substance were determined to be 5.576±0.004, 11.496±0.007, 1.340±0.005 kJ mol^{-1} and 99.30 mol%, respectively, on the basis of the heat capacity measurements. The molar entropies of the three phase transitions were calculated to be 16.550±0.012, 33.071±0.029 and 3.447±0.027 J mol^{-1} K^{-1}, respectively. Further researches of the thermochemical properties for this compound have been carried out by means of TG and DSC techniques. © 2000 Elsevier Science B.V. All rights reserved.

Keywords: Trifluoroacetamide; Heat capacity; Adiabatic calorimetry; Phase transition; Purity determination; TG; DSC

1. Introduction

Trifluoroacetamide ($C_2H_2F_3NO$) is a kind of important raw material used in the process of syntheses of many medicines and insecticides. Recently, due to its high enthalpies of phase transition, noncorrosiveness and good thermal stability, it has begun to be considered as a kind of energy-storage material in the aircraft. In 1923, B. Beim [1] used trifluoroacetic acid and saturated ammonia water as reactants and successfully synthesized the compound under the temperature of 10°C. He reported that the melting point and boiling point of the compound were determined to be 74.8 and 162.5°C, respectively. Since then, the reports about thermochemical properties of the substance were not found in the literature. For the application of the compound, thermodynamic data of this substance has urgently been required. In the present work, low temperature heat capacity measurements were carried out with adiabatic calorimetry, and the basic thermodynamic parameters, such as molar enthalpies and entropies of various phases transitions as well as chemical purity and thermal stability of the substance were determined on the basis of heat capacity measurements. Thermal stability of the compound was also studied by thermogravimetry (TG) and differential scanning calorimetry (DSC).

---

[*] Corresponding author. Fax: +86-411-4691570.
E-mail address: tzc@ms.dicp.ac.cn (Z.-C. Tan)

PII: S0040-6031(00)00479-2

2. Experimental

2.1. Sample

Trifluoroacetamide is a white crystal with a sheet crystalline shape. Its molecular formula is CF_3CONH_2. The sample used for the present calorimetric study was produced by Koch–Light Limited (Haverhill, Suffolk, UK). The labelled chemical purity is >99.0%. Its actual purity was determined by HPLC (Model: Simazu. 10A) analysis to be higher than 99.20 mol%. Its melting point was determined to be 74.2–74.9°C with the microscopic melting point device (Model: BY-1, Yazawa Co., Japan).

2.2. Adiabatic calorimetry

The heat capacity measurements were made by a precision automatic adiabatic calorimetric system for small sample over the temperature range from 78 to 404 K. The construction of the calorimeter has been described previously in detail in the literature [2]. It briefly consists of a sample cell, a thermometer, a heater, two adiabatic shields, two sets of eight-junction chromelcopel thermocouples and a high vacuum system. The calorimeter cell was made of gold-plated copper with internal volume of 6 cm^3. A miniature platinum resistance thermometer made by the Shanghai Institute of Industrial Automatic Meters, China, was used to measure the temperature of the calorimeter cell. The thermometer with an uncertainty of <1 mK (absolutely) was calibrated on the basis of the ITS-90 by the station of Low Temperature Metrology, Chinese Academy of Sciences. The thermometer was placed in the copper sheath at the bottom of the sample cell. After loading the sample into the cell, the upper cover and body of the cell were sealed together with a special kind of cycleweld. The cell was evacuated to within 10^{-3} Pa and then a small amount of helium gas was introduced through a copper capillary on the upper cover into the cell to improve the heat transfer. The sample cell was sealed with the tin solder after the copper capillary was pinched off from the tube end. Two adiabatic shields surrounded the cell and controlled its temperature. The whole calorimetric system was kept in a high vacuum with residual pressure of 10^{-3} Pa to obtain good adiabatic conditions.

The mass of the sample loaded in sample cell of the adiabatic calorimeter amounted to 4.0316 g, which was equivalent to 0.03567 mol based on its molar mass of 113.0395 g/mol.

The molar heat capacities of α-Al_2O_3 used as the standard substance were measured in the same temperature range as that of the sample measurement in order to confirm the reliability of the calorimeter. Deviations of the experimental results from those of the smoothed curve lie within ±0.2%, while the inaccuracy is within ±0.5%, as compared with those of the National Bureau of Standards [3] over the whole temperature range.

2.3. Differential scanning calorimetry (DSC)

A V4.0B DU Pont TA 2000 Thermal Analysis System coupled with a personal computer loaded with the program for processing the obtained results was used. The DSC measurements were carried out by a differential scanning calorimeter with aluminium sample pans and sapphire reference material. Both the sample and sapphire were scanned at a heating rate of 5 K min^{-1} under nitrogen atmosphere with a flow rate of 35 ml min^{-1}. The mass of the sample used for experiment was 4.3620 mg.

2.4. Thermogravimetry (TG)

A thermal analysis system equipped with a JF-2 thermobalance, a platinum wire furnace and two sets of platinum–rhodium thermocouples was used for the thermogravimetric measurements. The experiment was carried out in a nitrogen atmosphere with a sample of 11.9036 mg, a nitrogen flow rate of 25 ml min^{-1} and a linear heating rate of 10 K min^{-1}, respectively.

3. Results and discussion

3.1. Heat capacity

The low-temperature experimental molar heat capacities for trifluroacetamine are shown in Fig. 1 and listed in Table 1. The C_p–T curve in Fig. 1 indicates that there is no thermal anomaly over the temperature range from 78 to 326 K, which means that

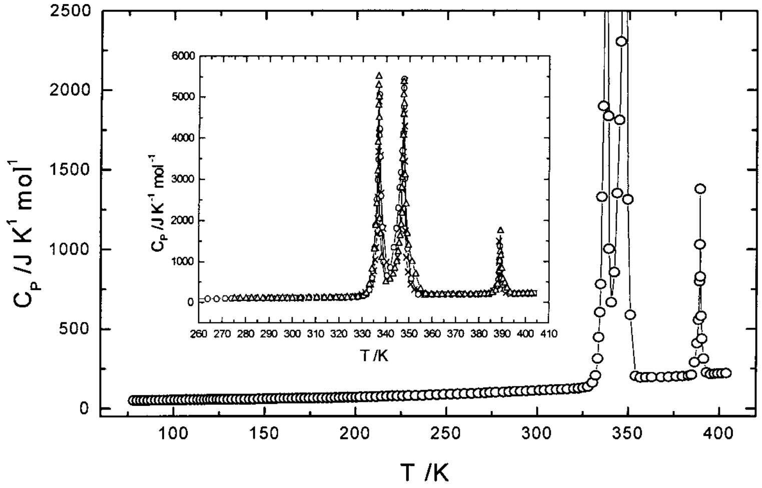

Fig. 1. Relation curve of heat capacities vs. temperature (C_p~T) of trifluoroacetamide ($C_2H_2F_3NO$) obtained by adiabatic calorimetry. The first series of heat capacity measurements represents (○); the second series of heat capacity measurements (Δ); the third series of heat capacity measurements (×).

Table 1
Experimental molar heat capacities of trifluoroacetamide ($C_2H_2F_3NO$) crystal (M=113.0395 g mol^{-1})

T/K	$C_{p,m}$/J K^{-1} mol^{-1}	T/K	$C_{p,m}$/J K^{-1} mol^{-1}	T/K	$C_{p,m}$/J K^{-1} mol^{-1}
Series 1					
78.281	49.306	191.285	67.168	336.137	2507.4
80.236	49.486	193.518	67.792	336.578	2987.2
82.251	49.827	195.825	68.391	336.801	3485.9
84.125	50.015	198.132	68.991	336.942	4076.8
86.176	50.065	200.413	69.633	337.031	5065.7
88.198	50.213	202.624	70.232	337.208	4233.0
90.399	50.336	205.587	70.875	337.553	3548.0
92.491	5 1.035	208.493	72.116	337.943	2592.9
94.668	51.122	211.405	72.716	338.481	1835.5
96.787	51.593	214.422	73.957	339.043	1002.8
98.803	52.064	217.384	75.199	340.440	666.82
100.987	52.800	220.239	76.440	341.990	857.65
103.019	52.957	223.045	76.879	343.443	1350.6
105.023	53.157	226.085	77.181	344.563	1811.8
107.006	53.526	229.136	77.682	345.378	2304.7
109.252	53.994	233.075	78.924	345.928	2795.7
111.342	54.124	236.974	80.165	346.478	3171.4
113.469	54.393	240.851	82.675	346.963	3692.2
115.355	54.709	244.797	84.174	347.397	4125.5
117.145	54.827	248.537	85.731	347.543	4763.6
118.857	54.991	252.377	87.572	347.569	5224.8
120.573	55.264	256.169	89.456	347.628	5445.6
122.215	55.575	259.933	90.889	348.178	3016.5
124.081	55.816	263.755	91.988	349.298	1311.8
125.856	56.069	267.591	93.486	350.898	587.46
127.785	56.334	271.299	95.514	353.945	202.35
130.048	56.441	274.019	97.376	356.617	192.06
132.248	56.461	277.201	99.239	359.795	193.53

Table 1 (*Continued*)

T/K	$C_{p,m}$/J K^{-1} mol^{-1}	T/K	$C_{p,m}$/J K^{-1} mol^{-1}	T/K	$C_{p,m}$/J K^{-1} mol^{-1}
134.561	56.578	281.413	101.11	362.851	194.49
136.962	56.601	284.549	102.96	368.082	195.86
139.388	56.942	287.679	104.84	372.238	197.06
141.780	57.446	290.879	105.72	376.394	200.01
144.110	57.917	294.080	107.59	379.753	201.94
146.699	58.938	297.280	109.45	383.066	204.77
149.118	59.364	301.152	111.35	384.647	210.82
151.518	59.734	303.924	113.17	386.312	290.26
153.815	60.276	307.298	114.89	387.563	407.49
156.179	61.044	310.611	116.73	388.309	554.88
158.558	61.644	313.545	118.50	388.805	800.01
160.887	61.315	316.478	120.28	388.916	1030.6
163.132	61.819	320.201	122.40	388.997	1378.4
165.355	62.291	322.750	124.99	389.187	829.82
167.699	62.795	325.281	127.58	389.743	581.39
170.097	63.318	327.837	134.63	390.232	437.64
172.327	63.573	330.293	159.63	391.209	312.87
174.731	63.771	332.012	205.69	392.929	225.79
177.101	64.242	333.099	312.84	395.205	213.73
179.505	64.904	333.568	444.95	397.406	215.84
181.909	65.090	334.081	604.59	399.252	218.13
184.367	65.217	334.549	782.11	401.452	219.96
186.674	65.688	335.109	1328.7	403.652	221.74
188.982	66.664	335.674	1897.5		
Series 2					
275.176	98.431	336.670	5290.6	357.109	210.69
277.692	99.313	336.709	5508.2	359.503	195.93
280.109	100.89	336.784	5003.0	361.991	196.02
282.503	101.74	336.902	4502.5	364.209	197.90
284.997	102.28	337.218	2047.1	366.681	198.76
287.392	104.63	337.708	1683.4	369.010	199.01
289.703	105.07	338.286	1105.1	371.557	199.72
291.103	105.88	340.054	503.07	374.019	199.97
293.478	106.73	341.889	571.69	376.437	200.91
295.793	107.71	343.178	696.46	378.724	202.08
297.880	108.91	343.912	843.85	380.793	203.21
300.013	109.78	344.644	1002.9	382.280	205.47
303.507	111.90	345.279	1240.8	384.112	213.58
306.993	115.01	345.745	1445.4	385.614	235.09
310.402	117.47	346.112	1626.0	387.129	295.20
313.689	118.09	346.557	1905.4	388.015	450.09
316.172	119.32	346.958	2185.8	388.593	780.23
318.687	121.52	346.751	2797.2	388.787	1023.4
321.109	124.79	346.964	3047.9	388.964	1247.7
323.501	126.46	347.041	3502.5	389.108	1749.3
325.891	127.96	347.223	4070.3	389.324	1149.1
328.109	135.23	347.325	4579.6	389.695	837.31
330.493	165.19	347.403	5059.7	390.221	573.19
331.719	223.90	347.457	5374.7	391.091	482.05
332.907	449.01	347.674	4842.0	392.127	350.37
334.108	823.05	348.159	3109.5	393.325	247.03
335.101	1309.1	348.694	2398.7	395.233	215.07
335.659	1880.5	349.184	1680.1	397.109	214.49

Table 1 (*Continued*)

T/K	$C_{p,m}$/J K^{-1} mol^{-1}	T/K	$C_{p,m}$/J K^{-1} mol^{-1}	T/K	$C_{p,m}$/J K^{-1} mol^{-1}
336.101	2406.8	349.803	1392.9	398.940	216.86
336.490	3202.4	351.301	1002.3	400.796	219.38
336.504	3901.5	352.901	701.93	402.507	221.09
336.596	4802.1	354.890	333.09		
Series 3					
293.311	106.87	336.993	4899.7	361.693	195.08
296.672	108.06	337.093	4109.2	364.209	195.67
299.901	109.39	337.446	3580.1	366.809	195.94
303.402	112.36	337.992	2667.3	369.458	196.36
306.830	114.45	338.840	1805.9	372.019	198.01
310.193	116.46	340.327	992.05	374.694	199.80
313.492	118.78	341.899	620.91	377.198	201.06
316.708	119.18	343.441	854.01	379.609	203.10
320.192	120.49	345.009	1109.2	381.993	205.11
322.013	125.80	345.901	1800.4	384.209	208.89
324.019	127.07	346.599	2290.7	386.103	276.38
326.091	139.32	346.992	2749.3	387.464	322.99
327.902	152.35	347.147	3152.3	388.095	497.01
329.706	201.57	347.390	3663.8	388.303	672.39
331.292	245.09	347.599	4094.3	388.492	990.20
332.689	314.37	347.690	4592.4	388.582	1499.2
333.672	447.34	347.782	5402.9	388.695	1034.0
334.303	580.32	347.889	4302.1	388.994	703.86
334.990	780.33	348.022	3441.7	389.477	412.09
335.404	1052.7	348.380	1752.3	390.390	332.49
335.874	1347.9	348.779	1105.9	391.562	245.26
336.208	1679.0	349.591	750.92	393.493	211.03
336.398	2047.8	350.693	448.04	395.494	213.88
336.532	2563.4	352.219	315.99	397.508	215.68
336.653	3019.5	354.345	278.02	399.604	217.99
336.779	3673.4	356.577	200.89	401.692	218.98
336.910	4126.2	359.103	194.70	403.589	220.82

the thermochemical properties of this compound is stable at temperatures below 326 K. However, there are three phase transitions over the temperature range from 326 to 393 K. The C_p-T curves in the range of three phase transitions are also plotted in Fig. 1.

Since melting point of this compound is about 74.50°C (=347.65 K) according to the results obtained with the microscopic melting point device and from the literature [1], this temperature agrees with the peak temperature of the second peak in C_p-T curve. Therefore, the second peak (T_m=347.622 K) is caused by the fusion of trifluroacetamide. Hence, it is obvious that the first peak corresponds to the solid–solid phase transition between two kinds of different crystal structures of the substance. The third peak occurring after melting may correspond to a phase transition from a kind of liquid crystalline phase to fully liquid phase. In accordance with the concept of liquid crystal phase [4], the liquid crystal may be produced from relatively long rod-shaped molecules with polar groups. Trifluroacetamide belongs to this kind of molecules. This phase transition is a kind of a transition from mesomorphic state to normal liquid state. In addition, this kind of liquid crystalline phase is formed partly because strong intermolecular hydrogen bonds between F, O or N atoms with large electronegativity and H atoms with small electronegativity exist among molecules of this kind of material and enhance the orderly degree of the molecules. So, the state of the substance over the temperature range from 350 to 388 K may belong to that of liquid crystalline phase.

It is noted from the above analysis that there are three stable phase stages in C_p–T curve, which are fully solid phase interval from 78 to 326 K, mesomorphic liquid crystalline phase stage from 362 to 385 K and fully liquid phase interval from 395 to 404 K, respectively, in the sequence of temperature increment. The values of experimental heat capacities in the three regions can be fitted to the following polynomial equations with least squares method:

1. For fully solid phase

$$\frac{C_{p,m}}{\mathrm{J\,K\,mol^{-1}}} = 70.043 + 33.178X + 22.484X^2 + 5.229X^3 - 8.076X^4 + 0.516X^5 + 3.628X^6$$

   in which $X=[(T/\mathrm{K})-202]/124$. The equation is valid from 78 to 326 K with an accuracy of ±0.25%.

2. For mesomorphic liquid crystalline phase

$$\frac{C_{p,m}}{\mathrm{J\,K\,mol^{-1}}} = 196.517 + 7.137X + 1.973X^2 - 6.134X^3 + 2.437X^4 + 9.916X^5$$

   in which $X=[(T/\mathrm{K})-370]/15$. The equation is valid from 355 to 385 K with an accuracy of ±0.2%.

3. For fully liquid phase

$$\frac{C_{p,m}}{\mathrm{J\,K\,mol^{-1}}} = 218.391 + 4.597X - 2.504X^2 - 0.333X^3 + 2.071X^4$$

   in which $X=[(T/\mathrm{K})-399.5]/4.5$. The equation is valid from 395 to 404 K with an accuracy of ±0.2%.

3.2. Molar enthalpies and entropies of phase transitions

The heat capacity measurements in the phase transition range were repeated three times in order to verify the truth of the three phase transitions. Before every series of experiment was carried out, the sample was cooled from 404 K to lower than 293 K with different cooling rates respectively, which included liquid-nitrogen (for first series, about 20 K min^{-1}), natural (for second series, about 0.2 K min^{-1}) and ice-water (for third series, about 5 K min^{-1}) cooling. The results of three series of repeated measurements have shown that all the three phase transitions possessed good repeatability and reversibility, no supercooled and other thermal anomaly phenomena caused by different cooling rates were observed in the course of heat capacity measurements. A satisfactory agreement in temperatures and C_p values of each series of repeated experiment was obtained. The results of three phase transitions obtained from every series of repeated experiments have been listed in Table 2. The molar enthalpies ΔH_m of the first and second phase transitions in $C_{p,m}$–T curve were calculated with the method of diagrammatic area integration because the two peaks were partly folded together. The molar enthalpy ΔH_m of the third phase transition was evaluated in terms of Eq. (1), and molar entropies ΔS_m of all three phase transitions were calculated with the following thermodynamic Eq. (2):

$$\Delta H_m = \frac{\left[Q - n\int_{T_i}^{T_m} C_{P(LC)} - n\int_{T_m}^{T_f} C_{P(L)}\,\mathrm{d}T - \int_{T_i}^{T_f} H_0\,\mathrm{d}T\right]}{n} \times (\mathrm{kJ\,mol^{-1}}) \tag{1}$$

$$\Delta S_m = \frac{\Delta H_m}{T_m} \quad (\mathrm{kJ\,mol^{-1}\,K^{-1}}) \tag{2}$$

Where T_i in Eq. (1) is a temperature slightly below the starting phase transition temperature; T_f a temperature slightly higher than the finishing phase transition temperature; $C_{P(C)}$ the average heat capacity at the temperature $(T_i+T_m)/2$; $C_{P(L)}$ the average heat capacity at the temperature $(T_m+T_f)/2$; Q the total heat quantity introduced to the calorimeter from temperature T_i to T_f; T_m the melting point of the sample measured; n the mole number of the sample; H_0 the heat capacity of the empty sample cell.

Values of Q and H_0 were calculated with the program stored in the computer linked with the adiabatic calorimetric system, and printed along with experimental results of heat capacities. Molar enthalpy ΔH_m and entropy ΔS_m of third phase transition calculated from Eqs. (1) and (2) are basically identical with those (1.338±0.004 kJ mol^{-1} and 3.441±0.020 J mol^{-1} K^{-1}, respectively) obtained with the method of diagrammatic area integration.

Table 2
Thermodynamic properties of three phase transitions obtained from three series of repeated heat capacity measurements of trifluoroacetamide ($C_2H_2F_3NO$)[a]

Thermodynamic properties	Series 1	Series 2	Series 3	Mean value	Standard deviation
	x_1	x_2	x_3	$\bar{x}$	σ_a[b]
$T_{tr,1}$/K	337.031	336.709	336.993	336.911	0.102
T_m/K	347.628	347.457	347.782	347.622	0.094
$T_{tr,2}$/K	388.997	389.108	388.582	388.896	0.160
$\Delta_{tr}H_{m,1}$/kJ mol^{-1}	5.582	5.577	5.569	5.576	0.004
$\Delta_{fus}H_m$/kJ mol^{-1}	11.494	11.509	11.486	11.496	0.007
$\Delta_{tr}H_{m,2}$/kJ mol^{-1}	1.338	1.349	1.334	1.340	0.005
$\Delta_{tr}S_{m,1}$/J K^{-1} mol^{-1}	16.562	16.563	16.526	16.550	0.012
$\Delta_{fus}S_m$/J K^{-1} mol^{-1}	33.064	33.124	33.026	33.071	0.029
$\Delta_{tr}S_{m,2}$/J K^{-1} mol^{-1}	3.440	3.467	3.433	3.447	0.027

[a] '$T_{tr,1}$/K, T_m/K and $T_{tr,2}$/K', '$\Delta_{tr}H_{m,1}$/kJ mol^{-1}, $\Delta_{fus}H_m$/kJ mol^{-1} and $\Delta_{tr}H_{m,2}$/kJ mol^{-1}', '$\Delta_{tr}S_{m,1}$/J mol^{-1} K^{-1}, $\Delta_{fus}S_m$/J mol^{-1} K^{-1} and $\Delta_{fus}S_{m,2}$/J mol^{-1} K^{-1}' are the peak temperatures, molar enthalpies and molar entropies of the first, second and third phase transitions, respectively.

[b] $\sigma_a = \sqrt{\sum_{i=1}^{n}(x_i - \bar{x})^2/n(n-1)}$ in which n is experimental number (n=3); x_i experimental value of each series of repeated measurement; $\bar{x}$ mean value.

3.3. Melting point and purity

The purity of the sample was evaluated from a set of equilibrium melting temperatures and melting fractions corresponding to these temperatures [4,5]. According to the ideal solution law, the relation between the mole fraction N ($N \ll 1$) of a small amount of impurities in the sample and its melting point can be expressed as follows:

$$N = \frac{\Delta_{fus}H_m(T_0 - T_1)}{RT_0^2} \tag{3}$$

in which T_0 is the melting point of an absolutely pure substance; T_1 the melting point of the given sample (strictly speaking, T_0 and T_1 should be the triple points under the experimental adiabatic condition); $\Delta_{fus}H_m$ the mole enthalpy of fusion; R the molar gas constant. As for the liquid solution formed by a part of the sample melted, given that N' is the mole fraction of the impurities and T melting point of the solution, then

$$N' = \frac{\Delta_{fus}H_m(T_0 - T_1)}{RT_0^2}. \tag{4}$$

Assuming that the impurities are solid-insoluble, namely, no solid-solution would be formed and all of the impurities can transfer completely into the liquid phase when the melting started, the relative amount of the sample in the liquid phase will increase in the process of the melting. On the other hand, since the total amount of the impurities is constant, the mole fraction of the impurities in the liquid phase will gradually decrease. Given that F is the ratio of the sample in the liquid phase to the total amount, then

$$F = \frac{q}{Q} \tag{5}$$

in which F is also designed as the melting fraction and its value is the ratio of the partial heat (q) required to melt a part of the sample to the total heat (Q) required melting the whole sample. Obviously, F is inversely proportional to the mole fraction of the impurities in the liquid phase, that is,

$$N' = \frac{1}{F}N. \tag{6}$$

Substituting Eqs. (4) and (5) into Eq. (6), the following equation can be obtained

$$T_0 - T = \frac{1}{F}(T_0 - T_1) \tag{7}$$

Eq. (7) suggests that the relationship between the equilibrium melting temperature T and the reciprocal of melting fraction $1/F$ is linear. Plotting T versus $1/F$, and extrapolating the straight line to $1/F$=1 and $1/F$=0, T_1 and T_0 can be derived (Fig. 2). The results are

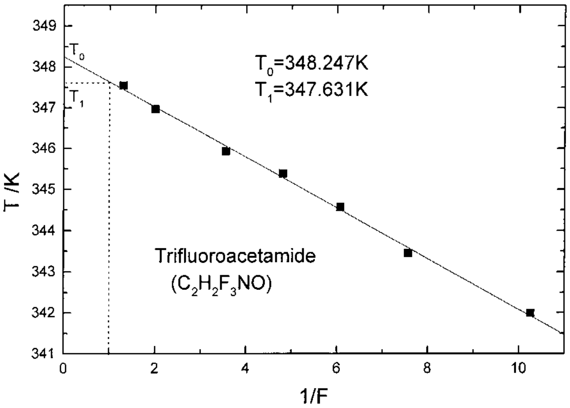

Fig. 2. Melting curve ($T\sim1/F$) of trifluoroacetamide ($C_2H_2F_3NO$).

tabulated in Table 3 and plotted in Fig. 2, where T_1=347.631 K and T_0=348.247 K are obtained. The melting point (T_1=347.631 K) agrees well with that (T_m=347.622±0.102 K) obtained from the heat capacity measurements as described earlier. In terms of Eq. (3), $N=7.02\times10^{-3}$ mol is evaluated. The purity of the sample is $1-N$=99.30 mol%.

3.4. DSC and thermogravimetric analysis

It can be seen from the DSC curve (Fig. 4) that there are three endothermic processes in the temperature range from 320 to 395 K. The temperature ranges and peak values of the three endothermic processes correspond to those of the three phase transitions in C_p-T curve obtained from the heat capacity measurements. This result also confirms that there are three phase transitions in the temperature range from 320 to 395 K for the compound, which include a solid-to-solid phase transition, a fusion and a phase transition from liquid crystalline phase to fully liquid phase.

Table 3
The experimental results of melting fractions (F) and equilibrium temperature (T) of trifluoroacetamide ($C_2H_2F_3NO$) $F=[q/(\Delta H_m n)]$

q/J	F	$1/F$	T/K
39.993	0.0975	10.2532	341.990
54.193	0.1322	7.5667	343.443
67.519	0.1647	6.0733	344.563
85.311	0.2081	4.8066	345.378
115.446	0.2815	3.5520	345.928
204.882	0.4996	2.00 14	346.963
315.196	0.7687	1.3001	347.543

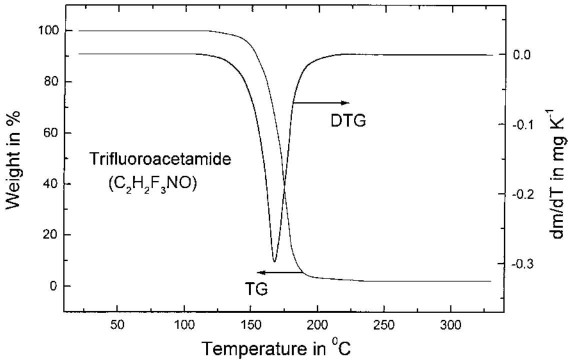

Fig. 3. TG and DTG curves of trifluoroacetamide ($C_2H_2F_3NO$).

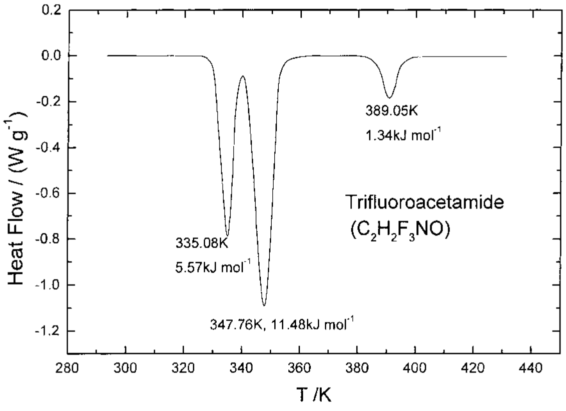

Fig. 4. DSC curve of trifluoroacetamide ($C_2H_2F_3NO$).

The curve of thermogravimetric analysis is shown in Fig. 3. It shows that no mass-loss process takes place before the temperature reaches about 155°C. Over the temperature range from 155 to 185°C, there is a single mass-loss stage. It is clear from DTG curve that the temperature corresponding to the maximum differential mass-loss percentage is about 164.7°C. In accordance with the literature [1], the boiling point of trifluroacetamide is about 162.4°C. Therefore, the mass-loss process is really due to the evaporation of the sample.

Acknowledgements

This work was financially supported by the Natural Science Foundation of China under the contract NSFC No. 29773048.

References

[1] B. Beim, BL. Acad. Belgique 5(8) (1923) 358; C (1923) I, 66, (from Beilstein No. 2^2, 186).

[2] Z.C. Tan, G.Y. Sun, A.X. Yin, W.B. Wang, J.C. Ye, L.X. Zhou, J. Therm. Anal. 45 (1995) 59.

[3] D.A. Ditmars, S. Ishihara, S.S. Chang, G. Bernstein, E.D. West, J. Res. Natl. Bur. Stand 87 (1982) 159.

[4] Z.Y. Zhang, M. Frenkel, K.N. Marsh, R.C. Wilhoit, Landolt-Bornstein, Thermodynamic Properties of Organic Compounds and their Mixtures, Group IV, Vol. 8, Subvolume A, Springer, Berlin, 1995 (Chapter 7).

[5] J.H. Badley, J. Phys. Chem. 63 (1959) 1991–1996.